J. Fluid Mech. (1976), *vol.* 78, *part* 3, *pp.* 621–637
Printed in Great Britain

On the dynamics of finite-amplitude baroclinic waves as a function of supercriticality

By JOSEPH PEDLOSKY

Department of the Geophysical Sciences, University of Chicago, Illinois 60637

(Received 14 June 1976)

A finite-amplitude model of baroclinic instability is studied in the case where the cross-stream scale is large compared with the Rossby deformation radius and the dissipative and advective time scales are of the same order. A theory is developed that describes the nature of the wave field as the shear supercriticality increases beyond the stability threshold of the most unstable cross-stream mode and penetrates regions of higher supercriticality. The *set* of possible steady nonlinear modes is found analytically. It is shown that the steady cross-stream structure of each finite-amplitude mode is a function of the supercriticality.

Integrations of initial-value problems show, in each case, that the final state realized is the state characterized by the finite-amplitude mode with the largest equilibrium amplitude. The approach to this steady state is oscillatory (non-monotonic). Further, each steady-state mode is a well-defined mixture of *linear* cross-stream modes.

1. Introduction

The important insight in fluid mechanics gained from analytical studies of the finite-amplitude dynamics of unstable perturbations is usually obtained only at the cost of restrictive parametric assumptions. Chief among these is the limitation that the supercriticality of the flow, i.e. the degree of *linear* instability, is small. In this limiting case the small linear destabilization can be matched by possible nonlinear stabilization well within a systematic small (but finite) amplitude perturbation theory. Although this quantitative restriction is limiting, it still provides a fruitful framework for the understanding of important nonlinear phenomena. In the meteorologically and oceanographically important problem of baroclinic instability it has provided important information about the mechanism and nature of the finite-amplitude stabilization process within a systematic and easily understood formalism (e.g. Drazin 1970; Pedlosky 1970, 1971; Hart 1973).

However, an important consequence of the restriction to small supercriticalities is that, except in unusual circumstances, only the threshold of the most unstable mode can be crossed. The marginal-stability curves of the less unstable modes are usually sufficiently distant from the corresponding neutral curve for the most unstable mode that the less unstable modes rapidly damp in the presence of viscosity. They therefore play little role in the dynamics.

The purpose of this paper is to consider a situation where, within the systematic formalism of weakly nonlinear dynamics, *several* instability thresholds can be crossed. This allows an examination of the finite-amplitude dynamics of flow states that are supercritical to *several* modes of motion. It is then possible to discuss the various finite-amplitude steady states that are theoretically possible and their relative stability. At least in so far as this multiple supercriticality is concerned, such a situation may be helpful in *understanding* the nonlinear dynamics of perturbations not limited by weak instability.

The problem considered is the finite-amplitude dynamics of a baroclinic wave in a viscous fluid in a channel whose width L is large compared with the Rossby radius of deformation (a length scale which characterizes the stable vertical density gradient). For a *fixed* downstream wave number† the stability criterion (see below) depends weakly (but non-trivially) on the cross-stream mode structure. The most unstable disturbance has the gravest cross-stream mode shape, while each of the higher cross-stream harmonics is slightly more stable. In this parameter limit it is then possible to examine supercritical states which are unstable to several cross-stream modes.

For supercriticalities small enough such that only the first mode is slightly unstable, the basic structure of the mode is determined by linear theory. For greater supercriticality the very structure of the cross-stream eigenmode, as well as its amplitude, is shown to be determined by nonlinear effects. The structure of the steady eigensolutions is dominated by a balance of linear and nonlinear effects which tend to reduce the cross-stream variation except (for larger supercriticalities) in narrow highly nonlinear regions.

For the problem considered here, detailed calculations of several initial-value problems show that, in the presence of viscosity, the final, finite-amplitude state is found to be that associated with the mode whose linear growth rate is largest. The approach to this steady state is *oscillatory* rather than monotonic as is the case for small supercriticality.

2. The model

The model considered is the two-layer model introduced by Phillips (1951) modified by the presence of viscous Ekman layers on the bounding horizontal surfaces. The reader is referred to Pedlosky (1970) for a detailed derivation of the appropriate equations in the quasi-geostrophic (rapidly rotating) limit. Suffice it to say that the model consists of two layers of homogeneous fluid, each with a different uniform density. These layers lie on a horizontal plane rotating with angular velocity Ω. The lighter fluid lies above the denser. The fluid is bounded above and below by rigid horizontal planes separated by a distance D. The interface between the two fluids is considered for simplicity to be equidistant from the two horizontal planes in the absence of motion. The fluid is confined laterally to a channel infinite in length and whose width is L.

† This choice is made for two reasons: it produces a tractable, interesting and mathematically consistent problem; and experimental observations (e.g. Hart 1973) suggest the importance of finite-amplitude states (steady and fluctuating) with this property.

The basic state whose stability is to be investigated is chosen to be the shear flow consisting of a rectilinear horizontally uniform flow in the upper layer with an equal but oppositely directed flow in the lower layer. The earlier studies referenced in the introduction indicate that this provides a realistic model for baroclinic instability and its finite-amplitude evolution.

The non-dimensional equations governing the *disturbance* fields can be shown to be (Pedlosky 1970)

$$\left(\frac{\partial}{\partial t}+\frac{U_s}{2}\frac{\partial}{\partial x}\right)[\nabla^2\psi_1-F(\psi_1-\psi_2)]+FU_s\frac{\partial\psi_1}{\partial x}+r\nabla^2\psi_1+J(\psi_1,\nabla^2\psi_1-F(\psi_1-\psi_2))=0, \tag{2.1a}$$

$$\left(\frac{\partial}{\partial t}-\frac{U_s}{2}\frac{\partial}{\partial x}\right)[\nabla^2\psi_2-F(\psi_2-\psi_1)]-FU_s\frac{\partial\psi_2}{\partial x}+r\nabla^2\psi_2+J(\psi_2,\nabla^2\psi_2-F(\psi_2-\psi_1))=0. \tag{2.1b}$$

In these equations subscripts 1 and 2 refer to variables defined for the upper and lower layers respectively. Scales L, U and L/U have been used to scale horizontal lengths, horizontal velocity and time, respectively. Distance down the channel is measured by x and distances across the channel by y, with corresponding velocities u_n and v_n. These horizontal velocities are obtained from the perturbation stream function $\psi_n(x,y,t)$ by

$$u_n=-\partial\psi_n/\partial y, \quad v_n=\partial\psi_n/\partial x. \tag{2.2a,b}$$

The effects of viscosity which appear in (2.1) are a consequence of the action of Ekman layers on the horizontal bounding surfaces and are given by the terms $r\nabla^2\psi_n$ in (2.1), where

$$r=E^{\frac{1}{2}}/\epsilon. \tag{2.3}$$

Here E is the Ekman number, ϵ the Rossby number defined by

$$E=\nu/\Omega D^2, \quad \epsilon=U/2\Omega L, \tag{2.4a,b}$$

where ν is the fluid's kinematic viscosity. The ratio r will throughout this paper be considered an $O(1)$ quantity. The nonlinearity in (2.1) is given by the Jacobian of the stream function and the potential vorticity in each layer, that is

$$J(a,b)\equiv\frac{\partial a}{\partial x}\frac{\partial b}{\partial y}-\frac{\partial a}{\partial y}\frac{\partial b}{\partial x}. \tag{2.5}$$

A crucial parameter in (2.1) is

$$F=\frac{4\Omega^2L^2}{\frac{1}{2}g(\Delta\rho/\rho)D}=L^2/R^2, \tag{2.6}$$

where $\Delta\rho/\rho$ is the fractional density difference between the two layers. F is the square of the ratio of the channel width L and the Rossby deformation radius

$$R=\frac{1}{2\Omega}\left(g\frac{\Delta\rho}{\rho}\tfrac{1}{2}D\right)^{\frac{1}{2}}.$$

In this paper we shall examine cases where F is large compared with 1. The basic state consists of the shear flow

$$u_1=\tfrac{1}{2}U_s=-u_2, \tag{2.7}$$

where U_s is a constant. Thus $u_1+u_2=0$ while $U_s=u_1-u_2$ for the basic state.

The appropriate boundary conditions for (2.1) are (Pedlosky 1970)

$$\partial\psi_n/\partial x = 0 \quad (y = 0, 1) \tag{2.8}$$

for the wave portion of the disturbance, with the complementary condition

$$\partial^2\psi_n/\partial y\,\partial t = 0 \quad (y = 0, 1) \tag{2.9}$$

for corrections to the x-independent velocity field.

3. Mathematical formulation

Linear stability theory (Pedlosky 1970) shows that the basic state given in (2.7) will be unstable with respect to disturbances of the form

$$\psi_n = A_n e^{ik(x-ct)} \sin\, m\pi y + * \tag{3.1}$$

(where * represents the complex conjugate of the preceding term) if U_s exceeds the critical value U_c, where

$$\tfrac{1}{2}U_c = rak^{-1}(2F - a^2)^{-\frac{1}{2}} \quad (a^2 < 2F) \tag{3.2}$$

and

$$a^2 = k^2 + m^2\pi^2. \tag{3.3}$$

In (3.1), m is any integer greater than zero. For given r, k and F, the lowest value of U_c occurs for $m = 1$. Higher cross-stream modes are always *more* stable according to linear theory. In general kc is given by the relation

$$kc = -\frac{ir(a^2+F)}{a^2+2F} + \frac{i}{a^2+2F}\left[k^2\frac{U_s^2}{4}(4F^2 - a^4) + r^2F^2\right]^{\frac{1}{2}}. \tag{3.4}$$

The threshold for instability of the basic state is given by the neutral-stability curve corresponding to $m = 1$, so that

$$U_c = 2ra_1 k^{-1}(2F - a_1^2)^{-\frac{1}{2}}, \tag{3.5}$$

where

$$a_1^2 = k^2 + \pi^2. \tag{3.6}$$

If U_s exceeds U_c by the small amount $U_c\Delta$, it follows from (3.4) that the growth rate $-ikc$ is given to $O(\Delta^2)$ by

$$-\frac{ikc}{r} = +\frac{(a^2+F)}{a^2+2F}\left[-1 + \left\{1 + \frac{2(2F+a^2)}{2F-a_1^2}\frac{[\Delta a_1^2(2F-a^2) - F(a^2-a_1^2)]}{(a^2+F)^2}\right\}^{\frac{1}{2}}\right]. \tag{3.7}$$

If $a^2 = a_1^2$, the growth rate will be positive. Since

$$a^2 - a_1^2 = (m^2 - 1)\pi^2, \tag{3.8}$$

the higher modes are less unstable, or even stable if Δ is not large enough, i.e. the mth mode will be stable if

$$\Delta < (m^2 - 1)\pi^2 F/a_1^2(2F - a^2). \tag{3.9}$$

The minimum critical shear, i.e. the minimum value of U_c as a function of k, occurs when

$$k^2 = \pi[(2F)^{\frac{1}{2}} - \pi], \tag{3.10}$$

for which value

$$U_c = 2r[(2F)^{\frac{1}{2}} - \pi]^{-1}. \tag{3.11}$$

Now consider the case† $F \gg 1$. As long as m is $O(1)$, it follows from (3.10) that for the most unstable waves

$$a^2 = O(k^2) = O(F^{\frac{1}{2}}). \tag{3.12}$$

According to (3.9) the magnitude of Δ required to cross the stability curve of the mth cross-stream mode is

$$\Delta = \Delta_m \cong 2^{-\frac{3}{2}}(m^2-1)\pi F^{-\frac{1}{4}} = O(F^{-\frac{1}{4}}). \tag{3.13}$$

Thus for large F the neutral curves of the *higher* cross-stream modes are penetrated by even *small* supercriticalities Δ as long as

$$F^{\frac{1}{4}}\Delta = O(1). \tag{3.14}$$

This will be the basic parameter setting of this study. These results suggest the following rescaling:

$$\xi = F^{\frac{1}{4}}x \quad \text{(from 3.10)}, \qquad T = \Delta F^{-\frac{1}{2}}t \quad \text{(from 3.7)}, \qquad U_c = \mathscr{U}_c F^{-\frac{1}{4}} \quad \text{(from 3.11)}. \tag{3.15a–c}$$

It is also convenient to introduce the functions

$$\psi_B = \tfrac{1}{2}F^{-\frac{3}{4}}(\psi_1+\psi_2), \quad \psi_T = \tfrac{1}{2}F^{-1}(\psi_1-\psi_2). \tag{3.16a,b}$$

Equations (2.1a, b) can then be put in the form

$$\begin{aligned}
&\frac{\mathscr{U}_c}{2}(1+\mu\sigma)\frac{\partial}{\partial\xi}\left(\frac{\partial^2}{\partial\xi^2}+\mu\frac{\partial^2}{\partial y^2}\right)\psi_T + r\left(\frac{\partial^2}{\partial\xi^2}+\mu\frac{\partial^2}{\partial y^2}\right)\psi_B \\
&\quad = -\mu^2\frac{\partial}{\partial T}\left(\frac{\partial^2}{\partial\xi^2}+\mu\frac{\partial^2}{\partial y^2}\right)\psi_B - \mu\left\{\frac{\partial\psi_T}{\partial\xi}\frac{\partial}{\partial y}\left(\frac{\partial^2\psi_T}{\partial\xi^2}+\mu\frac{\partial^2\psi_T}{\partial y^2}\right)\right. \\
&\quad\quad \left. -\frac{\partial\psi_T}{\partial y}\frac{\partial}{\partial\xi}\left(\frac{\partial^2\psi_T}{\partial\xi^2}+\mu\frac{\partial^2\psi_T}{oy^2}\right)\right\} - \mu^2\left\{\frac{\partial\psi_B}{\partial\xi}\frac{\partial}{\partial y}\left(\frac{\partial^2\psi_B}{\partial\xi^2}+\mu\frac{\partial^2\psi_B}{\partial y^2}\right)\right. \\
&\quad\quad \left. -\frac{\partial\psi_B}{\partial y}\frac{\partial}{\partial\xi}\left(\frac{\partial^2\psi_B}{\partial\xi^2}+\mu\frac{\partial^2\psi_B}{\partial y^2}\right)\right\}
\end{aligned} \tag{3.17a}$$

and

$$\begin{aligned}
&U_c(1+\mu\sigma)\frac{\partial\psi_B}{\partial\xi} + r\left(\frac{\partial^2}{\partial\xi^2}+\mu\frac{\partial y^2}{\partial^2}\right)\psi_T \\
&\quad = -\mu\frac{\mathscr{U}_c}{2}(1+\sigma\mu)\frac{\partial}{\partial\xi}\left(\frac{\partial^2}{\partial\xi^2}+\mu\frac{\partial^2}{\partial y^2}\right)\psi_B + \mu\frac{\partial}{\partial T}\left\{2\psi_T - \mu\left(\frac{\partial^2}{\partial\xi^2}+\mu\frac{\partial^2}{\partial y^2}\right)\psi_T\right\} \\
&\quad\quad + 2\mu\left(\frac{\partial\psi_B}{\partial\xi}\frac{\partial\psi_T}{\partial y} - \frac{\partial\psi_B}{\partial y}\frac{\partial\psi_T}{\partial\xi}\right) - \mu^2\left\{\frac{\partial\psi_B}{\partial\xi}\frac{\partial}{\partial y}\left(\frac{\partial^2\psi_T}{\partial\xi^2}+\mu\frac{\partial^2\psi_T}{\partial y^2}\right)\right. \\
&\quad\quad \left. -\frac{\partial\psi_B}{\partial y}\frac{\partial}{\partial\xi}\left(\frac{\partial^2\psi_T}{\partial\xi^2}+\mu\frac{\partial^2\psi_T}{\partial y^2}\right)\right\} - \mu^2\left\{\frac{\partial\psi_T}{\partial\xi}\frac{\partial}{\partial y}\left(\frac{\partial^2\psi_B}{\partial\xi^2}+\mu^2\frac{\partial\psi_B}{\partial y^2}\right)\right. \\
&\quad\quad \left. -\frac{\partial\psi_T}{\partial y}\frac{\partial}{\partial\xi}\left(\frac{\partial^2\psi_B}{\partial\xi^2}+\mu\frac{\partial^2\psi_B}{\partial y^2}\right)\right\},
\end{aligned} \tag{3.17b}$$

where

$$\sigma = \Delta F^{\frac{1}{4}}, \quad \mu = F^{-\frac{1}{2}}. \tag{3.18a,b}$$

† Formally, this limit is considered subsequent to the limits $\epsilon \to 0$, $E \to 0$.

The perturbation stream functions are now expanded in the series

$$\left.\begin{aligned}\psi_B &= \phi_B^{(0)}+\mu\phi_B^{(1)}+\mu^2\phi_B^{(2)}+\dots,\\ \psi_T &= \phi_T^{(0)}+\mu\phi_T^{(1)}+\mu^2\phi_T^{(2)}+\dots.\end{aligned}\right\} \tag{3.19}$$

This expansion is inserted in (3.17) and leads to a sequence of linear problems, the first of which, at order one, yields

$$\frac{\mathscr{U}_c}{2}\frac{\partial\phi_T^{(0)}}{\partial\xi}+r\phi_B^{(0)}=0, \quad \mathscr{U}_c\phi_B^{(0)}+r\frac{\partial\phi_T^{(0)}}{\partial\xi}=0, \tag{3.20a,b}$$

from which it follows that

$$\mathscr{U}_c = 2^{\frac{1}{2}}r, \quad \phi_B^{(0)} = -2^{-\frac{1}{2}}\partial\phi_T^{(0)}/\partial\xi. \tag{3.21), (3.22}$$

Thus, at this leading order only the asymptotic critical shear for large F and the relation between the barotropic and baroclinic perturbations are determined, as seen on comparing (3.5) with (3.21). The *structure* of the perturbation is still unknown.

The $O(\mu)$ problem yields, with the aid of (3.21) and (3.22),

$$2^{-\frac{1}{2}}\frac{\partial^3\phi_T^{(1)}}{\partial\xi^3}+\frac{\partial^2\phi_B^{(1)}}{\partial\xi^2} = -2^{-\frac{1}{2}}\sigma\frac{\partial^3\phi_T^{(0)}}{\partial\xi^3}-\frac{1}{r}\frac{\partial}{\partial\xi}\left(\frac{\partial\phi_T^{(0)}}{\partial\xi}\frac{\partial}{\partial y}\frac{\partial^2\phi_T^{(0)}}{\partial\xi}-\frac{\partial\phi_T^{(0)}}{\partial y}\frac{\partial^2\phi_T^{(0)}}{\partial\xi^2}\right), \tag{3.23a}$$

$$\begin{aligned}2^{-\frac{1}{2}}\frac{\partial^2\phi_T^{(1)}}{\partial\xi^2}+\frac{\partial\phi_B^{(1)}}{\partial\xi} &= 2^{-\frac{1}{2}}\sigma\frac{\partial^2\phi_T^{(0)}}{\partial\xi^2}-2^{-\frac{1}{2}}\frac{\partial^2\phi_T^{(0)}}{\partial y^2}+2^{-\frac{3}{2}}\frac{\partial^4\phi_T^{(0)}}{\partial\xi^4}+r\frac{\partial\phi_T^{(0)}}{\partial T}\\ &\quad+\sigma\frac{1}{r}\left(\frac{\partial\phi_T^{(0)}}{\partial\xi}\frac{\partial^2\phi_T^{(0)}}{\partial\xi\,\partial y}-\frac{\partial\phi_T^{(0)}}{\partial y}\frac{\partial^2\phi_T^{(0)}}{\partial\xi^2}\right).\end{aligned} \tag{3.23b}$$

At this stage, we look for solutions of the form

$$\phi_T^{(0)} = \Phi_T(y,T)+f(y,T)\,e^{i\alpha\xi}+*. \tag{3.24}$$

Thus the lowest-order solution consists of a slowly varying correction to the zonal flow plus a wave field with a single zonal wavenumber α but an arbitrary cross-stream structure.

If (3.24) is substituted into (3.23) and (3.23a) is integrated once with respect to ξ, subtraction of (3.23b) from (3.23a) yields *two equations*. One is for that part of the remainder that is independent of ξ, while the other is for that part which varies as $\exp(i\alpha\xi)$. Naturally both must vanish separately. The result is

$$\frac{1}{r}\frac{\partial\Phi_T}{\partial T}-\frac{1}{2}\frac{\partial^2\Phi_T}{\partial y^2} = -2^{-\frac{1}{2}}\alpha^2\frac{d}{dy}\frac{|f|^2}{r}, \tag{3.25}$$

$$\frac{1}{r}\frac{\partial f}{\partial T}-\frac{1}{2}\frac{\partial^2 f}{\partial y^2}-f\left(\sigma\alpha^2-\frac{\alpha^4}{4}\right)-\frac{2^{\frac{1}{2}}}{r}\alpha^2\frac{\partial\Phi_T}{\partial y}f=0. \tag{3.26}$$

Let
$$-\frac{\partial\Phi_T}{\partial y} = 2^{-\frac{3}{2}}\frac{s^2r}{\alpha^2}u(y,\tau), \quad f=\frac{sr}{2\alpha^2}\phi(y,\tau), \tag{3.27a,b}$$

where
$$s^2 = 2\alpha^2(\sigma-\tfrac{1}{4}\alpha^2), \quad \tau=\tfrac{1}{2}rT. \tag{3.28}$$

It then follows that (3.25) and (3.26) can be put in the more agreeable form

$$\frac{\partial\phi}{\partial\tau}-\frac{\partial^2\phi}{\partial y^2} = s^2\phi(1+u), \quad \frac{\partial u}{\partial\tau}-\frac{\partial^2 u}{\partial y^2}=\frac{\partial^2|\phi|^2}{\partial y^2}. \tag{3.29a,b}$$

These equations have a simple interpretation. The first, (3.29*a*), is the evolution equation for the baroclinic wave perturbation ϕ. The second represents the evolution in space and time of the correction to the mean zonal flow. This correction is produced by rectified transports of vorticity produced by the wave field and represented by the term on the right-hand side of (3.29*b*). This correction to the zonal flow changes the effective growth rate of the perturbation field and this effect is represented by the term on the right-hand side of (3.29*a*). The appropriate boundary conditions for (3.29*a*, *b*) are, from (2.8) and (2.9),

$$u = \phi = 0 \quad (y = 0, 1). \tag{3.30}$$

It is important to note that the cross-stream structure of the wave, as well as its evolution in time, is to be determined from (3.29). This is in contrast to the cases studied earlier (Pedlosky 1970), in which the cross-stream structure is determined by the linear problem for marginal stability. *In the case at hand the structure of the wave field is a function of its amplitude and will evolve with time.* Furthermore the problem is of *second* order in time rather than first order as is usually the case when $r = O(1)$ (Pedlosky 1970). This point will be discussed further below.

4. The linear and slightly supercritical problems

It is helpful to reconsider briefly the linear stability problem in the context of the system (3.29). For time intervals small enough that ϕ and u are still small, (3.29*a*) reduces to

$$\partial\phi/\partial\tau - \partial^2\phi/\partial y^2 = s^2\phi. \tag{4.1}$$

Solutions of (4.1) in the form

$$\phi_m = A \exp(\sigma_m t) \sin m\pi y$$

satisfy (3.29*a*) and (3.30) if

$$\sigma_m = s^2 - m^2\pi^2. \tag{4.2}$$

Hence the mth cross-stream mode is linearly unstable if $s > m\pi$. With the aid of (3.28), (3.21), (3.18) and (3.15*c*), it follows that the critical shear obtained when $s = m\pi$ is

$$U_c = \frac{2^{\frac{1}{2}} r}{F}\left(1 - \frac{k^2}{4F} + \frac{m^2\pi^2}{2k^2}\right), \tag{4.3}$$

where

$$k = \alpha F^{\frac{1}{4}}. \tag{4.4}$$

It is easy to verify that (4.3) is the large-F limit of (3.2), while (4.2) is the corresponding limit of (3.4). Hence if $s^2 > m^2\pi^2$ the cross-stream modes $\sin j\pi y$ with $1 \leqslant j \leqslant m$ are unstable, while cross-stream modes with $j > m$ are linearly stable. On the other hand, if s^2 only *slightly* exceeds the *first* critical bifurcation, i.e. if

$$s^2 = \pi^2 + \omega, \tag{4.5}$$

where

$$\omega \ll 1, \tag{4.6}$$

it follows that the growth rate will be small, $O(\omega)$, and that τ should be rescaled by $\theta = \omega\tau$. Doing so (3.9a, b) become

$$\omega\frac{\partial\phi}{\partial\theta}-\frac{\partial^2\phi}{\partial y^2} = (\pi^2+\omega)\phi(1+u), \quad \omega\frac{\partial u}{\partial\theta}-\frac{\partial^2 u}{\partial y^2} = \frac{\partial^2|\phi|^2}{\partial y^2}, \tag{4.7a,b}$$

from which it follows that, to lowest order in ω,

$$u = -|\phi|^2, \tag{4.8}$$

while to the same order

$$\phi = \omega^{\frac{1}{2}}A(\theta)\sin\pi y,$$

where $A(\theta)$ is seen to satisfy, after the usual (Pedlosky 1970) expansion process, the *first*-order equation

$$\frac{dA}{d\theta} = A-\frac{3\pi^2}{4}A|A|^2. \tag{4.9}$$

This leads to *monotonic* equilibration and a steady wave amplitude.

The essence of the considerations of the present study is the question of how this behaviour, which is standard for weak supercriticality, is altered when s^2 is sufficiently large that $\omega = O(1)$ or equivalently, when more than one linear mode is unstable. Clearly, only when ω is small will the cross-stream structure be determined independently of the amplitude behaviour. That is, when $s^2-\pi^2 = O(1)$, we are confronted with the strongly nonlinear problem (3.29) rather than the sequence of linear problems for the wave structure arising from (4.7).

5. Steady nonlinear modes

By linear theory, steady solutions are possible only when $s = \pi$. When s slightly exceeds this threshold (4.9) implies that eventually a steady wave of amplitude $2\times 3^{-\frac{1}{2}}(s^2/\pi^2-1)^{\frac{1}{2}}$ is achieved. In this section the nature of the finite-amplitude steady solutions for s arbitrarily greater than this first threshold are examined.

It follows from (3.29) and (3.30) that without loss of generality ϕ can be considered real. Further, in the steady problem

$$u(y) = -\phi^2(y), \tag{5.1}$$

so that $\phi(y)$ satisfies

$$d^2\phi/dy^2-s^2\phi(1-\phi^2) = 0, \quad \phi(0) = \phi(1) = 0. \tag{5.2}$$

Solutions of (5.2) which satisfy $\phi(0) = 0$ are (Byrd & Friedman 1971)

$$\phi(y) = A_0\,\mathrm{sn}\left(\frac{s}{\nu}\frac{A_0}{2^{\frac{1}{2}}}y;\,\nu\right), \tag{5.3}$$

where sn is the *Jacobian elliptic function* with *argument* $2^{-\frac{1}{2}}s\nu^{-1}A_0 y$ and modulus ν. The modulus and amplitude are related by the condition

$$A_0 = 2^{\frac{1}{2}}\nu(\nu^2+1)^{-\frac{1}{2}}. \tag{5.4}$$

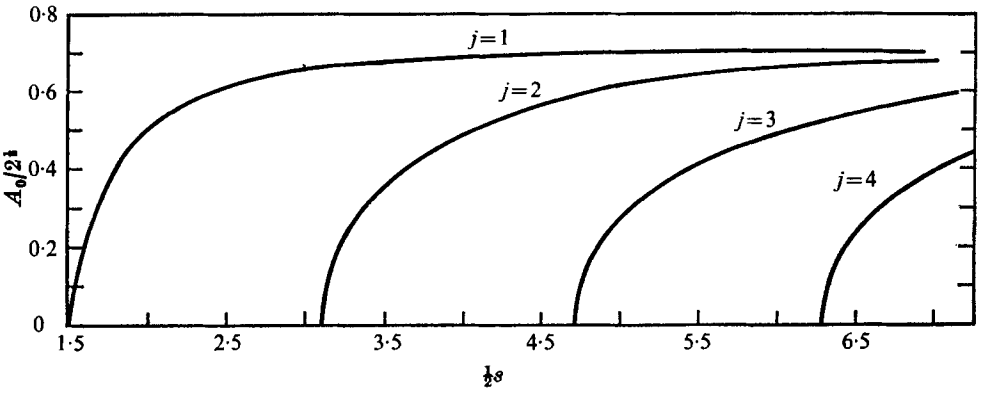

FIGURE 1. Bifurcation diagram showing the amplitude of the first four steady cross-stream modes as a function of supercriticality.

The function sn (x, ν) has its zeros at the points

$$x_j = 2jK(\nu) \quad (j = 1, 2, 3 \ldots), \tag{5.5}$$

where $K(\nu)$ is the complete elliptic integral,

$$K(\nu) = \int_0^{\frac{1}{2}\pi} (1 - \nu^2 \sin^2 \xi)^{-\frac{1}{2}} d\xi, \quad 0 \leqslant \nu \leqslant 1. \tag{5.6}$$

The condition $\phi(1) = 0$ is therefore satisfied only if

$$2^{-\frac{1}{2}} \frac{s}{\nu} A_0 = s(\nu^2 + 1)^{-\frac{1}{2}} = 2jK(\nu). \tag{5.7}$$

In the range $0 \leqslant \nu \leqslant 1$, $K(\nu)$ is a monotonically increasing function. Its minimum value at $\nu = 0$ is seen from (5.6) to be $\frac{1}{2}\pi$ and it logarithmically approaches infinity as $\nu \to 1$. It follows from (5.7), therefore, that, for each j, s must exceed $j\pi$ for a steady solution to exist. When this is compared with (4.3) it follows that, when s exceeds $j\pi$, exactly j nonlinear steady solutions are possible and these correspond to the crossing of the linear stability threshold of the jth linear cross-stream mode. For each j, (5.3) may be rewritten as

$$\phi(y) = A_0 \,\mathrm{sn}\,(2jK(\nu)\, y, \nu), \tag{5.8a, b}$$

where $A_0 = 2^{\frac{1}{2}}\nu(\nu^2 + 1)^{-\frac{1}{2}}$ and where $\nu(s)$ is determined from (5.7). The amplitude of the wave is therefore determined entirely as a function of s. The amplitudes of the first four steady solutions as a function of s are shown in figure 1. There are several important things to note about this amplitude diagram. As previously remarked, the number of steady solutions that are possible at a given value of s depends on the degree of supercriticality, i.e. the number of cross-stream modes that would be linearly unstable at that s. For values of $s > 2\pi$ more than one steady solution is always possible but not *simultaneously*. That is, *for $s > 2\pi$ at least two steady solutions exist, but no non-trivial linear superposition of these steady solutions will satisfy* (5.2). Thus, if the system evolves to a steady state it must choose between several possible equilibrium states.

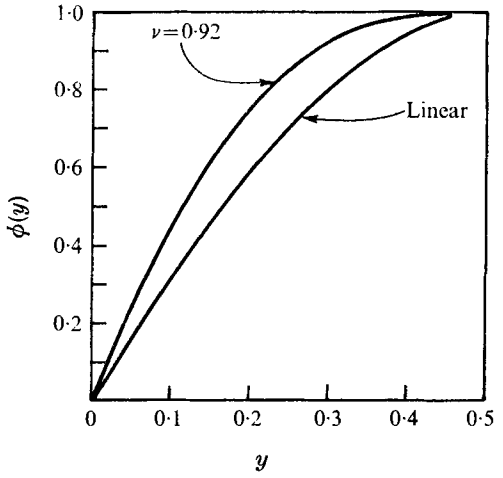

FIGURE 2. The spatial structure of the first cross-stream mode for $s = 6{\cdot}28$ ($\nu(s) = 0{\cdot}92$) compared with the linear sinusoidal mode ($0 \leqslant y \leqslant 0{\cdot}5$).

Furthermore, as is clear from figure 1, the amplitudes of the various possible steady solutions each approach unity as s becomes large. In fact, using the asymptotic form (Byrd & Friedman 1971) of $K(\nu)$ as $\nu \to 1$ ($s \gg 1$), it can be shown that, for $s \ll j\pi$, the amplitude of the wave mode is given by

$$A_{0_j} \sim 1 - \tfrac{3}{4}\exp\{-(s/j \times 2^{\frac{1}{2}} - 2{\cdot}772)\}. \tag{5.9}$$

It should be noted, however, that because of the rescaling implied by (3.27b) the actual amplitude of the wave is sA_{0_j}. Hence the amplitude difference between modes j and k is, for large s,

$$s(A_{0_j} - A_{0_k}) = -\tfrac{3}{4}s\{\exp[-(s/j \times 2^{\frac{1}{2}} - 2{\cdot}772)] - \exp[-(s/k \times 2^{\frac{1}{2}} - 2{\cdot}772)]\}. \tag{5.10}$$

Thus, asymptotically, for very large s the first few modes will have *nearly* identical amplitudes. However, even for moderately large s the amplitude differences are considerable. For example, for $s = 10$, for which value exceeds the stability threshold of the first three modes, $s(A_{0_1} - A_{0_2})$ is 1·233 or about 12 % of the larger amplitude.

The structure in y, as well as the *amplitude* of the nonlinear modes, is also a function of the supercriticality. For values of s that only slightly exceed the jth threshold, $s = j\pi$, the structure of the jth mode, from (5.8), is given by

$$\phi_j(y) = A_{0_j}\sin(j\pi y). \tag{5.11}$$

As s increases beyond this threshold the structure of the elliptic function distorts the simple sinusoidal character of the eigensolutions. Figure 2 shows the first cross-stream mode at a value of $s = 6{\cdot}28$. Note the tendency of the nonlinear mode to be *flatter* over the central portion of the channel and steeper near the boundaries. Figure 3 shows the cross-stream structure for an even more extreme value of $s = 15{\cdot}37$. This limiting behaviour for large s can be understood directly from (5.2). For large s, (5.2) indicates that *almost* everywhere $\phi^2 = 1$. This is in

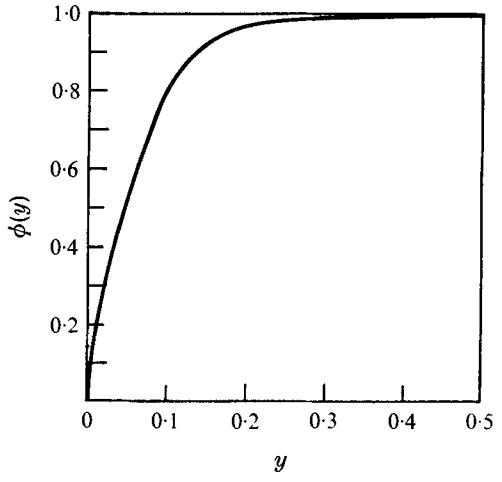

FIGURE 3. The spatial structure of the first cross-stream mode for $s = 15{\cdot}37$ ($\nu = 0{\cdot}99$) ($0 \leqslant y \leqslant 0{\cdot}5$).

agreement with the amplitude results discussed above and the tendency towards a *uniform distribution* of disturbance amplitude with y with increasing nonlinear effects. Naturally, since ϕ must vanish at $y = 0$ and $y = 1$, *narrow regions of rapid variation are observed near the walls*. These regions decrease their width inversely with s.

The higher modes with $j > 1$ have nodes at the positions

$$y_{jp} = p/j \quad (p = 0, 1, 2, \ldots, j), \tag{5.12}$$

i.e. precisely the same positions as those given by the *linear* solution (5.11). However, for each j, as s exceeds $j\pi$ by greater and greater amounts, the space between the nodes is characterized by regions of more and more uniform values of ϕ punctuated by narrow regions around the nodes where ϕ rapidly changes from $\phi = -1$ to $\phi = +1$. Fairly extreme values of s are required for this simple description to be very accurate. However, it does describe the tendency of the nonlinear effects to distort the modal structure.

An alternate way of characterizing the nonlinear steady modes is in terms of their harmonic content. That is, given the vanishing of ϕ at $y = 0$ and 1, each nonlinear mode can appropriately be expanded in a sine series, each term of which is individually a mode of the linear problem.

The following definitions are standard and useful:

$$\nu^1 = (1-\nu^2)^{\frac{1}{2}}, \quad K^1 = K(\nu^1), \quad q(\nu) = \exp(-\pi K^1/K). \tag{5.13}$$

Furthermore it is known that (Byrd & Friedman 1971)

$$\mathrm{sn}\,(x, \nu) = \frac{2\pi}{\nu K(\nu)} \sum_{m=0}^{\infty} \frac{q^{m+\frac{1}{2}}}{1-q^{2m+1}} \sin\left[(2m+1)\frac{\pi x}{2K(\nu)}\right]. \tag{5.14}$$

	s	3·24		4·92		7·107		10·42	
ϕ_{11}	ϕ_{21}	0·277	0	0·9116	0	1·088	0	1·182	0
ϕ_{12}	ϕ_{22}	0	0	0	0	0	0·507	0	0·9454
ϕ_{13}	ϕ_{23}	$1·25 \times 10^{-3}$	0	0·0498	0	0·130	0	0·2325	0
ϕ_{14}	ϕ_{24}	0	0	0	0	0	0	0	0
ϕ_{15}	ϕ_{25}	$3·2 \times 10^{-7}$	0	0·0028	0	0·018	0	0·0598	0
ϕ_{16}	ϕ_{26}	0	0	0	0	0	0·005	0	0·0591

TABLE 1. The harmonic content of the steady solutions

In the present case this yields

$$\phi_j(y) = \frac{2^{\frac{3}{2}} j\pi}{s} \sum_{m=0}^{\infty} \frac{q^{m+\frac{1}{2}}}{(1-q^{2m+1})} \sin(2m+1) j\pi y \tag{5.15}$$

$$\equiv \sum_{K=1}^{\infty} \phi_{jK} \sin K\pi y.$$

Since $q(\nu)$ is a tabulated function of ν while ν is a function of s through (5.7), the harmonic content ϕ_{jK} of the jth mode can easily be determined at each s. Some examples are shown in table 1, where the first six harmonics are tabulated for $j = 1$ and 2.

Table 1 shows that for slight supercriticalities, for example, for

$$s = 3·24 = \pi + 0·1,$$

the harmonic content of the first mode, which is the only possible mode, is almost entirely in its first harmonic. The second harmonic of the first mode is always identically zero, while the third harmonic ϕ_{13} is very small, i.e. $O(10^{-3})$. On the other hand for large supercriticalities, e.g. $s = 10·42$ (for which $(s-s_c)/s_c = 2·316$, where $s_c = \pi$), the harmonic content of both the first and second nonlinear modes is richer. For the first mode the third harmonic is now 20 % of the first harmonic. The second mode is almost entirely given by the second harmonic. The sixth harmonic (the second mode's next non-trivial harmonic) has only 6 % of the amplitude of the second. Thus, even for fairly large supercriticalities, the steady solutions are represented quite accurately by the first half-dozen Fourier harmonics.

Naturally, there is no *a priori* guarantee that these steady solutions are relevant. It is conceivable, especially where more than one steady solution is possible, that either all or all but some of the steady solutions are unstable. In the former case the solutions to the initial-value problem would remain time-dependent while in the latter case only the *stable* steady solution(s) would be realizable. To answer these questions it is necessary to return to the time-dependent set (3.29).

6. The time-dependent problem

In order to study the time-dependent problem, it is useful to transform (3.29) to spectral form, writing

$$\phi(y,\tau) = \sum_{K=1}^{\infty} \phi_K(t) \sin K\pi y, \quad u(y,\tau) = \sum_{K=1}^{\infty} u_K(t) \sin K\pi y. \qquad (6.1a,b)$$

Then (3.29) can be turned to an infinite set of ordinary differential equations for the spectral amplitudes $\phi_K(\tau)$, $u_K(\tau)$, viz.

$$\frac{d\phi_K}{d\tau} + K^2\pi^2\phi_K = s^2\phi_K - s^2 \sum_{m=1}^{\infty}\sum_{n=1}^{\infty} \phi_m u_n q_{Kmn}, \qquad (6.2a)$$

$$\frac{du_K}{d\tau} + K^2\pi^2 u_K = K^2\pi^2 \sum_{m=1}^{\infty}\sum_{n=1}^{\infty} \phi_m \phi_n q_{Kmn}, \qquad (6.2b)$$

where
$$q_{Kmn} = \frac{4}{\pi} \frac{Kmn}{(K^2-(m-n)^2)(K^2-(m+n)^2)} [1-(-1)^{K+m+n}]. \qquad (6.3)$$

In fact, guided by necessity and the results of the steady problem, the infinite sums in (6.2a, b) are truncated such that

$$1 \leqslant m \leqslant N, \quad 1 \leqslant n \leqslant N. \qquad (6.4)$$

The resulting set of $2N$ ordinary differential equations was integrated numerically by a Runge–Kutta scheme. The time τ was discretized such that each time step corresponded to an interval in τ of $\Delta\tau/\pi^2$. For most of the calculation, $\Delta\tau$ was chosen to be 0·01 and $N = 6$. As a test case in two of the calculations $\Delta\tau$ was halved while in another N was doubled to 12. In no case was a significant difference in the numerical results obtained. In the interpretation of the results it is useful to keep in mind that each *nonlinear* mode consists of a subset of the Fourier modes, e.g. the first nonlinear mode is made up of the first, third and fifth (etc.) and it is the lowest Fourier mode in each subset which dominates. Thus in the figures presented below only the dominant Fourier components of each of the nonlinear modes are presented.

7. Results

Figure 4 presents the results of a calculation for which $\frac{1}{2}s = 2{\cdot}0$, so that while the system is quite supercritical with respect to the first mode, $(s-s_c)/s_c = 33\,\%$, it is still considerably subcritical with respect to the second mode. In this calculation the first Fourier harmonic rapidly attains its equilibrium value as determined from figure 1. There is, however, a slight overshoot of the amplitude $\phi_1(t)$. The amplitude of the second mode, stable by linear theory, rapidly diminishes to zero.

Figure 5 presents the results of a calculation at a higher supercriticality ($\frac{1}{2}s = 3{\cdot}49$) for which *both* the first and second Fourier modes are *linearly* unstable. Figure 5 shows that ϕ_1 and ϕ_3 eventually attain their steady-state values (labelled A_{1e} and A_{3e} respectively) appropriate to the *nonlinear*, steady, *first* mode. On

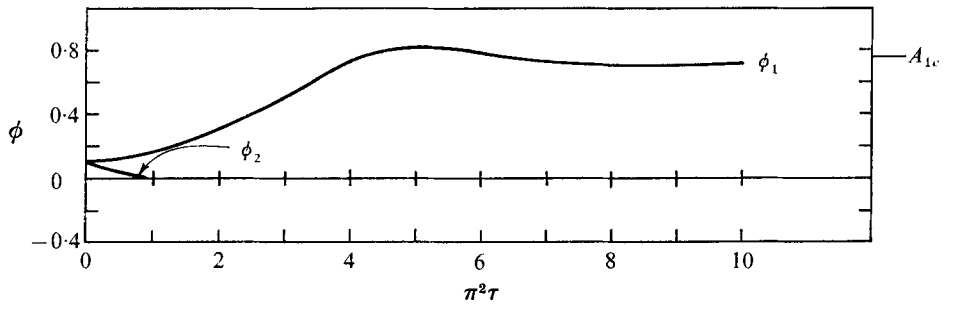

FIGURE 4. The amplitude of the first two Fourier harmonics as a function of time for $s = 4$. Note the approach of ϕ_1 to its equilibrium value and the decay of ϕ_2. Only the first nonlinear mode is a possible steady solution for this value of s.

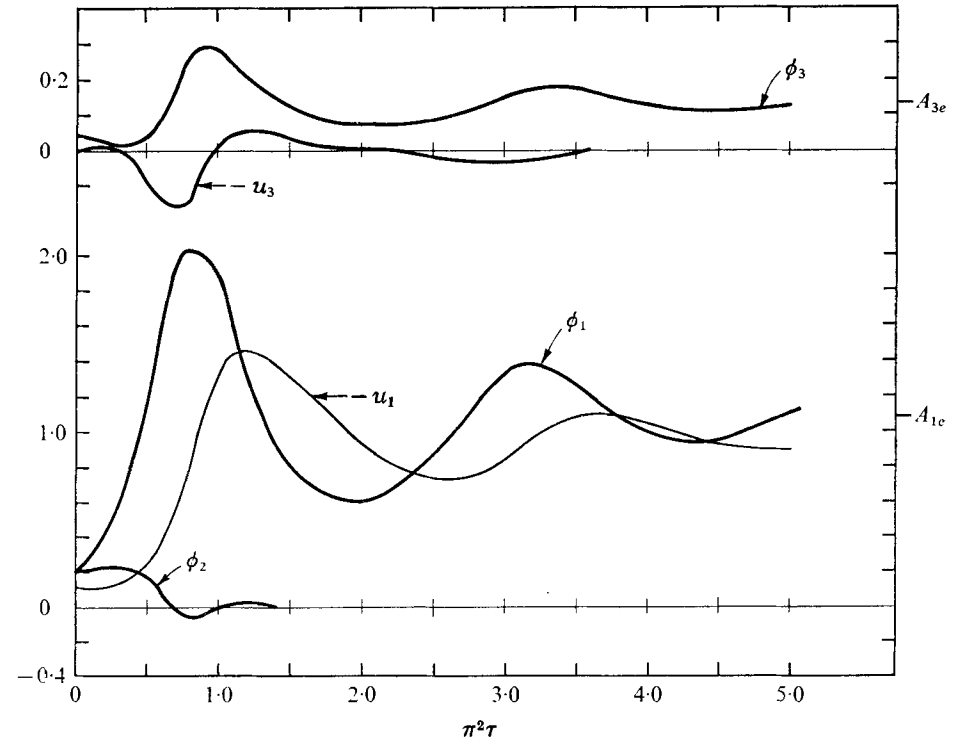

FIGURE 5. The time histories of ϕ_1, ϕ_2, ϕ_3, u_1 and u_3 as a function of time. Note the non-monotonic approach of the Fourier components of the first nonlinear mode to their equilibrium values and the decay of the second mode. $s = 6{\cdot}98$.

the other hand, $\phi_2(t)$, which well represents the amplitude of the second possible nonlinear mode, rapidly diminishes to zero. The solution has converged to the first nonlinear mode.† Thus the mode which is most unstable according to linear theory, or equivalently, has the largest nonlinear steady-state amplitude is the one realized as the solution to the initial-value problem. Figure 5 also

† This was further checked by doubling the range of integration in t.

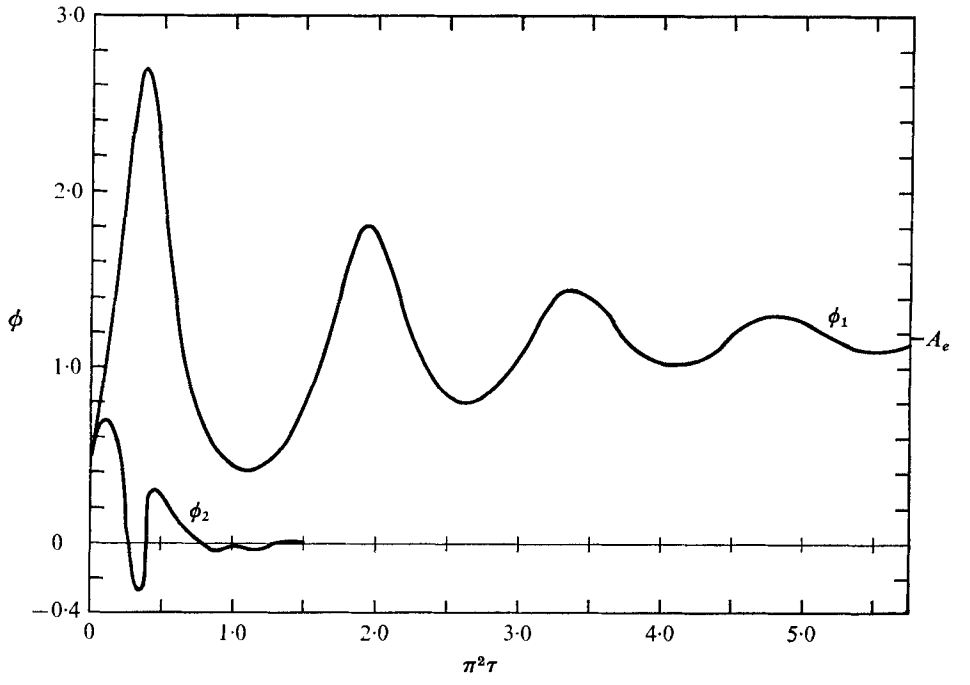

FIGURE 6. The time histories of ϕ_1 and ϕ_2. $s = 10{\cdot}43$. Note the increased oscillation, though damped, for this larger s.

shows the time history of the zonal flow corrections $u_1(t)$ and $u_3(t)$. It is interesting and important to note that the progress towards equilibration is now no longer monotonic. The evolution in time is considerably oscillatory and the oscillations only gradually damp to the steady solution. Further, there is considerable overshoot of the equilibrium amplitudes. It is also interesting to note that ϕ_1 and ϕ_3 oscillate in phase with each other.

This oscillatory behaviour, it is clear, is a function of the increasing supercriticality since, as was shown in (4.9), for this region of parameter space very slight supercriticality would produce monotonic equilibration of the classical Landau type.

Figure 6 shows the results of a calculation at yet a higher supercriticality ($\frac{1}{2}s = 5{\cdot}219$). At this value of s the first three cross-stream modes are linearly unstable. Once again the solution converged to the first nonlinear steady mode, after considerable oscillation. This is a particularly important case, because for this s, as figure 1 shows, the amplitudes of the first two nonlinear modes are fairly similar. Nonetheless, the solution converged to the mode favoured by nonlinear steady theory with the larger amplitude. This particular calculation was checked by doubling the truncation level to 12 for both ϕ_K and u_K with no alteration in the results.

An attempt was made to see whether the second nonlinear mode might be conditionally stable in the sense that initial conditions 'close' to the second nonlinear mode might be maintained with time. In figure 6 both ϕ_1 and ϕ_2 had

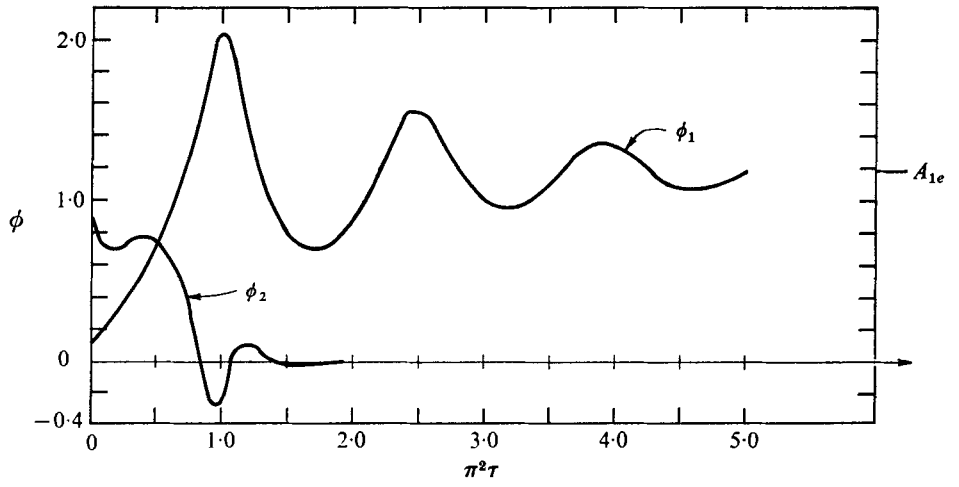

FIGURE 7. The time histories of ϕ_1 and ϕ_2 for the same supercriticality as in figure 6 ($s = 10{\cdot}43$). In this case $\phi_2(0) \gg \phi_1(0)$. The evolution of ϕ_1 to its equilibrium value and the rapid disappearance of ϕ_2 show the relative instability of the second nonlinear mode with respect to the first.

equal initial conditions. For the same value of s the experiment was repeated with ϕ_1 having only about 10 % of the amplitude of ϕ_1. Within a time $\pi^2\tau = 0{\cdot}5$, ϕ_1 surpassed ϕ_2 in amplitude and reached the same asymptotic limit, namely, the absence of the second nonlinear mode and the final emergence of the steady, first nonlinear mode.

It is difficult to 'prove' anything with only numerical calculations, but the suggestion is inescapable. Although the nature of the equilibration is non-monotonic, and oscillatory, the solutions, even for considerable supercriticality, converge to the first nonlinear mode as calculated analytically. The higher nonlinear modes seem unstable with respect to the first. It should be kept in mind, however, that the first (indeed each) nonlinear mode is a mixture of Fourier modes. In that sense the end state is a mixed *Fourier* mode state whose harmonic content is determined by (5.15).

8. Conclusions

Earlier studies referenced in the introduction have shown that when the ratio of the dissipation to advective time scales for the fluid is $O(1)$, weakly nonlinear theory predicts a monotonic approach to a final equilibrium state. The baroclinic wave in that state for such substantial dissipation has a spatial structure determined by linear theory and is a simple Fourier mode. The present study has allowed a considerable extension of the dynamics to cases where the supercriticality is large enough so that several modes are unstable.

The main result herein is that the baroclinic waves converge in time to the finite-amplitude solution with the largest steady-state amplitude. This nonlinear mode is a 'mixed-mode'† in the sense described by Lorenz (1963) but this is

† That is, containing several linear modes.

merely because each separate nonlinear mode consists of a spectrum of Fourier modes.

Experiments by Hart (1973) showed that continual fluctuations or limit cycles were found for systems too viscous to support the limit-cycle behaviour found by Pedlosky (1971) for small supercriticality. The present theory also does not yield such *continuing* fluctuations. The emergence, however, of (ephemeral) oscillatory behaviour in these *substantially* dissipative cases encourages the following speculation. It is possible that the present large-F analysis, redone for smaller dissipation, might yield limit-cycle behaviour when the small supercriticality theory (Pedlosky 1971) is yet still too viscous. This notion is encouraged by the fact that Hart has observed these fluctuations at large F. This problem is being studied further.

This study was partially supported by a grant from the Atmospheric Sciences section of the National Science Foundation.

REFERENCES

Byrd, P. F. & Friedman, M. D. 1971 *Handbook of Elliptic Integrals for Engineers and Scientists*. Springer.

Drazin, P. G. 1970 Non-linear baroclinic instability of a continuous zonal flow. *Quart. J. Roy. Met. Soc.* **96**, 667–676.

Hart, J. E. 1973 On the behavior of large-amplitude baroclinic waves. *J. Atmos. Sci.* **30**, 1017–1034.

Lorenz, E. N. 1963 The mechanics of vacillation. *J. Atmos. Sci.* **20**, 448–464.

Pedlosky, J. 1970 Finite amplitude baroclinic waves. *J. Atmos. Sci.* **27**, 15–30.

Pedlosky, J. 1971 Finite-amplitude baroclinic waves with small dissipation. *J. Atmos. Sci.* **28**, 587–597.

Pedlosky, J. 1972 Limit cycles and unstable baroclinic waves. *J. Atmos. Sci.* **29**, 53–63.

Phillips, N. A. 1951 A simple three-dimensional model for the study of large scale extra tropical flow pattern. *J. Met.* **8**, 381–394.